NUSC Report No. NL-3030

The Open-Circuit Sensitivity of Radially Polarized Ferroelectric Ceramic Hollow Spheres

CHARLES L. LEBLANC
Sonar Transducer Division

14 December 1970

NAVAL UNDERWATER SYSTEMS CENTER
New London Laboratory

REVIEWED AND APPROVED: 14 December 1970

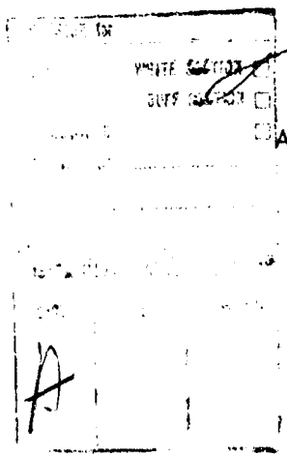

W. A. Von Winkle
Associate Technical Director
for Research
New London Laboratory

Correspondence concerning this report should be addressed as follows:

Officer in Charge
New London Laboratory
Naval Underwater Systems Center
New London, Connecticut 06320

ABSTRACT

The open-circuit sensitivities of radially polarized ferroelectric ceramic spheres are derived from the viewpoint of treating the ceramic as an anisotropic material. The results are in good agreement with similar sensitivities predicted on the basis of isotropic stress distributions. Graphs of the open-circuit sensitivity versus the ratio of wall thickness to outside diameter for several different ceramic materials indicate the region over which the spherical elements may be considered to be thin-walled spheres. Included for comparison are the sensitivities of similar ceramic spheres that are not pressure-released on the inside surface but are in immediate contact with a solid sphere. Also included are graphs of the magnitude of the stresses induced in the spheres by the ambient hydrostatic pressures.

ADMINISTRATIVE INFORMATION

This study was performed under New London Laboratory Project No. A-509-00-00, "Use of Blanket Hydrophones for Submarine Noise Studies" (U), Principal Investigator, J. Libuha, Code 2112, Special Developments Branch, Submarine Sonar Division, and Navy Subproject and Task No. SF 35 452 007-12970 (Partial), Program Manager, A. Paladino, NAVSHIPS 03722.

The technical reviewer for this report was Dr. R. S. Woollett, Code 2221, research consultant to the Sonar Transducer Division.

TABLE OF CONTENTS

REVERSE BLANK

LIST OF TABLES

LIST OF ILLUSTRATIONS

REVERSE BLANK

THE OPEN-CIRCUIT SENSITIVITY OF RADIALLY POLARIZED FERROELECTRIC CERAMIC HOLLOW SPHERES

INTRODUCTION

For a proper comparison of different hydrophone designs, it was deemed necessary to investigate the open-circuit sensitivity of radially polarized ferroelectric ceramic hollow spheres. The analysis included the material anisotropy, which, in the limit of very thin shells, does not influence the sensitivity values. Graphs of the open-circuit sensitivity versus the ratio (R) of wall thickness to outside diameter indicate the range over which the spheres may be considered to be thin-walled vessels. Included also are graphs of the internal shell stresses resulting from ambient pressure loads.

THEORETICAL CONSIDERATIONS

Figure 1 depicts the spherical coordinate system that will be used in this investigation and a section of a hollow ceramic sphere. By convention, the principal directions of stress in the ceramic are designated by the axes 1, 2, and 3 and are chosen to coincide with the set of spherical coordinates θ, ϕ, and r, respectively. Axis 3 is parallel to the polarization vector (radial) in the ceramic sphere.

The strain components in spherical coordinates are given as[1]

$$S_1 = \frac{u_r}{r} + \frac{1}{r}\frac{\partial u_\theta}{\partial \theta} , \tag{1}$$

$$S_2 = \frac{u_r}{r} + \frac{u_\theta}{r}\cot\theta + \frac{1}{r \sin\theta}\frac{\partial u_\phi}{\partial \phi} , \tag{2}$$

$$S_3 = \frac{\partial u_r}{\partial r} , \tag{3}$$

$$S_4 = \frac{1}{r \sin\theta}\frac{\partial u_r}{\partial \phi} + \frac{\partial u_\phi}{\partial r} - \frac{u_\phi}{r} , \tag{4}$$

$$S_5 = \frac{\partial u_\theta}{\partial r} - \frac{u_\theta}{r} + \frac{1}{r}\frac{\partial u_r}{\partial \theta} \text{ , and} \tag{5}$$

$$S_6 = \frac{1}{r}\left(\frac{\partial u_\phi}{\partial \theta} - u_\phi \cot\theta\right) + \frac{1}{r \sin\theta}\frac{\partial u_\theta}{\partial \phi} \text{ .} \tag{6}$$

where the subscripts 1, 2, and 3 represent the normal components, subscripts 4, 5, and 6 represent the shear components, and u_θ, u_ϕ, and u_r are the particle displacements in the θ, ϕ, and r directions, respectively.

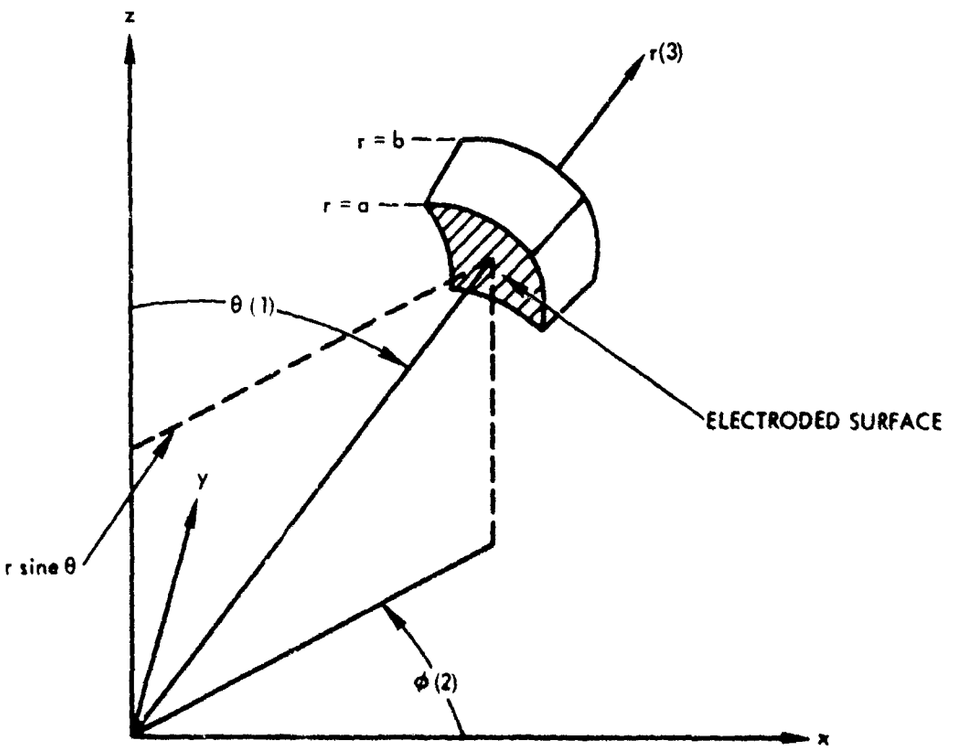

Fig. 1. Volume Element of a Hollow Ceramic Sphere

The equations of static equilibrium, excluding body forces, can be written as[2]

$$\frac{\partial T_3}{\partial r} + \frac{1}{r}\frac{\partial T_5}{\partial \theta} + \frac{1}{r \sin\theta}\frac{\partial T_4}{\partial \phi} + \frac{1}{r}\left(2T_3 - T_1 - T_2 + T_5 \cot\theta\right) = 0 \quad , \tag{7}$$

$$\frac{\partial T_5}{\partial r} + \frac{1}{r}\frac{\partial T_1}{\partial \theta} + \frac{1}{r \sin\theta}\frac{\partial T_6}{\partial \phi} + \frac{1}{r}\left[\left(T_1 - T_2\right)\cot\theta + 3T_5\right] = 0, \text{ and} \tag{8}$$

$$\frac{\partial T_4}{\partial r} + \frac{1}{r}\frac{\partial T_6}{\partial \theta} + \frac{1}{r \sin\theta}\frac{\partial T_2}{\partial \phi} + \frac{1}{r}\left[3T_4 + 2T_6 \cot\theta\right] = 0 \quad . \tag{9}$$

If the stress (T) and the electric displacement (D) are chosen as the independent variables, the constitutive equations of state can be written as

$$S_1 = s_{11}^D T_1 + s_{12}^D T_2 + s_{13}^D T_3 + g_{31} D_3 \quad , \tag{10}$$

$$S_2 = s_{12}^D T_1 + s_{11}^D T_2 + s_{13}^D T_3 + g_{31} D_3 \quad , \tag{11}$$

$$S_3 = s_{13}^D (T_1 + T_2) + s_{33}^D T_3 + g_{33} D_3 \quad , \tag{12}$$

$$S_4 = s_{44}^D T_4 + g_{15} D_2 \quad , \tag{13}$$

$$S_5 = s_{44}^D T_5 + g_{15} D_1 \quad , \tag{14}$$

$$S_6 = 2(s_{11}^D - s_{12}^D) T_6 \quad . \tag{15}$$

$$\mathcal{E}_1 = -g_{15} T_5 + \beta_{11}^T D_1 , \tag{16}$$

$$\mathcal{E}_2 = -g_{15} T_4 + \beta_{11}^T D_2 , \text{ and} \tag{17}$$

$$\mathcal{E}_3 = -g_{31} (T_1 + T_2) - g_{33} T_3 + \beta_{33}^T D_3 \quad , \tag{18}$$

where s^D is the elastic compliance coefficient at constant electric displacement, g is the piezoelectric coefficient, and β^T is the incremental impermeability at constant stress (T = 0).

Since the inside and outside surfaces of the sphere are fully electroded, it may be assumed that $D_1 = D_2 = 0$. In addition, spherical symmetry will be assumed so that the polar and azimuthal particle displacements (u_θ and u_ϕ, respectively) and any differentiations

with respect to the angular variables (θ and ϕ) can be neglected. It is, therefore, apparent that with these assumptions the shear strains (S_4, S_5, and S_6) can be set equal to zero and that, in turn, the shear stresses (T_4, T_5, and T_6) are zero also. It can also be concluded that the transverse electric fields ($\mathcal{E}_1$ and $\mathcal{E}_2$) are identically zero.

The usable (workable) strain relationships and equations of state reduce to

$$S_1 = s_{11}^D T_1 + s_{12}^D T_2 + s_{13}^D T_3 + g_{31} D_3 = \frac{u_r}{r} \quad , \tag{19}$$

$$S_2 = s_{12}^D T_1 + s_{11}^D T_2 + s_{13}^D T_3 + g_{31} D_3 = \frac{u_r}{r} = S_1 \quad , \tag{20}$$

$$S_3 = s_{13}^D (T_1 + T_2) + s_{33}^D T_3 + g_{33} D_3 = \frac{\partial u_r}{\partial r} \quad , \text{ and} \tag{21}$$

$$\mathcal{E}_3 = -g_{31} (T_1 + T_2) - g_{33} T_3 + \beta_{33}^T D_3 \quad , \tag{22}$$

whereas the equations of equilibrium degenerate to

$$\frac{\partial T_3}{\partial r} + \frac{1}{r}(2T_3 - T_1 - T_2) = 0 \text{ and } \frac{1}{r}(T_1 - T_2) \cot \theta = 0 \quad . \tag{23}$$

The last equation in the above set is satisfied when $T_1 = T_2$; thus the polar stress and the radial stress are related as follows:

$$T_1 = \frac{r}{2} T_3' + T_3 \text{ , or} \tag{24}$$

$$T_1' = \frac{r}{2} T_3'' + \frac{3}{2} T_3' \quad , \tag{25}$$

where the prime denotes $\partial/\partial r$.

Before proceeding further, let us look at some of the constraints imposed upon the electric displacement ($\vec{D}$) and the electric field ($\vec{\mathcal{E}}$). Maxwell's equations, neglecting the influence of the time rate of change of magnetic induction and the presence of local concentrations of free charge in the ceramic, require that the divergence of the electric displacement and the curl of the electric field be zero. In spherical coordinates, these constraints are expressed as

$$\vec{\nabla} \cdot \vec{D} = \frac{1}{r^2} \frac{\partial}{\partial r}(r^2 D_3) + \frac{1}{r \sin \theta} \frac{\partial}{\partial \theta}(D_1 \sin \theta) + \frac{1}{r \sin \theta} \frac{\partial D_2}{\partial \phi} = 0 \text{ , and} \tag{26}$$

$$\vec{\nabla} \times \vec{\mathcal{E}} = \frac{\vec{1}_r}{r^2 \sin\theta}\left[\frac{\partial}{\partial\theta}(r\mathcal{E}_2 \sin\theta) - \frac{\partial}{\partial\phi}(r\mathcal{E}_1)\right] + \frac{\vec{1}_\theta}{r\sin\theta}\left[\frac{\partial}{\partial\phi}(\mathcal{E}_3) - \frac{\partial}{\partial r}(r\mathcal{E}_2 \sin\theta)\right] + \frac{\vec{1}_\phi}{r}\left[\frac{\partial}{\partial r}(r\mathcal{E}_1) - \frac{\partial}{\partial\theta}(\mathcal{E}_3)\right] = 0 \quad , \tag{27}$$

where $\vec{1}_r$, $\vec{1}_\theta$, and $\vec{1}_\phi$ are unit vectors in the r, θ, and φ directions, respectively.

Since it has been previously stipulated that $D_1 = D_2 = 0$ and $\mathcal{E}_1 = \mathcal{E}_2 = 0$, then Maxwell's equations are satisified if

$$\frac{\partial}{\partial r}(r^2 D_3) = 0 \quad , \quad \frac{\partial \mathcal{E}_3}{\partial\phi} = 0 \quad , \text{and} \quad \frac{\partial \mathcal{E}_3}{\partial\theta} = 0 \quad . \tag{28}$$

The last two equations in the set, Eq. (28), require that $\mathcal{E}_3$ be independent of θ and φ. This complies with the spherical symmetry argument. The first equation of the above set is satisfied if

$$D_3 = \frac{A_o}{r^2} \quad . \tag{29}$$

Therefore, the electric charge (q) appearing on either electrode may be derived as

$$q = \int_A D_3 \, dA = \int_0^{2\pi}\int_0^{\pi} \frac{A_o}{r^2} r^2 \sin\theta \, d\theta \, d\phi = 4\pi A_o \quad , \tag{30}$$

which also defines the constant A_o .

Returning to the equations of state, we now determine the radial stress distribution. Since the polar and azimuthal strains (S_1 and S_2 , respectively) are equal, it is sufficient to work with only one of these strain equations. If Eq. (19) is used to define the radial particle displacement (u_r) and is differentiated once with respect to the radial coordinate, remembering that $T_1 = T_2$, then

$$\frac{\partial u_r}{\partial r} = \left(s_{11}^D + s_{12}^D\right) T_1 + s_{13}^D T_3 + R_{11} D_3 + r\left(s_{11}^D + s_{12}^D\right) T_1' + r s_{13}^D T_3' + r R_{11} D_3' \quad . \tag{31}$$

Equating Eq. (31) with Eq. (21) yields

$$\left(s_{11}^D + s_{12}^D - 2s_{13}^D\right) T_1 + \left(s_{11}^D - s_{13}^D\right) T_3 + r\left(s_{11}^D + s_{12}^D\right) T_1' + r s_{13}^D T_3' + r R_{11} D_3' + \left(R_{11} - R_{33}\right) D_3 = 0 \tag{32}$$

If Eqs. (24) and (25) are used to define T_1 and T_1' in terms of the radial stress and its derivatives, and if Eq. (29) is used to express the electric displacement and its derivative $\left(D_3' = -2A_o/r^3\right)$, then Eq. (32) can be reduced to

$$T_3'' + \frac{4}{r}T_3' + \frac{2}{r^2}T_3\left[1 - \frac{\left(s_{13}^D + s_{33}^D\right)}{\left(s_{11}^D + s_{12}^D\right)}\right] - \frac{2\left(g_{31} + g_{33}\right)}{r^4\left(s_{11}^D + s_{12}^D\right)}A_o = 0 \quad . \tag{33}$$

The complete solution of this nonhomogeneous, second-order differential equation consists of two parts, namely, the complementary solution and the particular solution. The complementary solution is found by choosing

$$T_{3(c)} = r^\alpha \sum_{n=o}^{\infty} c_n r^n \; ;$$

therefore,

$$T_{3(c)}' = r^\alpha \sum_{n=o}^{\infty} n c_n r^{n-1} + \alpha r^{\alpha-1} \sum_{n=o}^{\infty} c_n r^n, \text{ and}$$

$$T_{3(c)}'' = r^\alpha \sum_{n=o}^{\infty} (n-1) n c_n r^{n-2} + 2\alpha r^{\alpha-1} \sum_{n=o}^{\infty} n c_n r^{n-1} + (\alpha-1)\alpha r^{\alpha-2} \sum_{n=o}^{\infty} c_n r^n \quad .$$

Substituting these definitions into Eq. (33), with $A_o = 0$, yields

$$r^\alpha \sum_{n=o}^{\infty} \left\{\alpha^2 + \alpha(3+2n) + \left[n^2 + 3n + 2(1-\gamma)\right]\right\} c_n r^{n-2} = 0 \quad , \tag{34}$$

where

$$\gamma = \frac{\left(s_{13}^D + s_{33}^D\right)}{\left(s_{11}^D + s_{12}^D\right)} \; .$$

When Eq. (34) is expanded and the coefficient of successive powers of r is set equal to zero, we get the following sequence of equations:

$$r^\alpha \left[\alpha^2 + 3\alpha + 2(1-\gamma)\right] c_o r^{-2} = 0 \quad , \tag{35}$$

$$r^\alpha \left[\alpha^2 + 5\alpha + 2(3-\gamma)\right] c_1 r^{-1} = 0 \quad , \tag{36}$$

$$r^\alpha \left[\alpha^2 + 7\alpha + 2(6-\gamma)\right] c_2 r^o = 0 \quad , \tag{37}$$

$$r^\alpha \left[\alpha^2 + 9\alpha + 2(10-\gamma)\right] c_3 r^1 = 0, \quad \text{etc.} \tag{38}$$

The first of these equations, called the indicial equation, yields two values for α ; i.e,

$$\alpha_{1,2} = -\frac{3}{2} \pm \sqrt{\left(\frac{3}{2}\right)^2 - 2(1-\gamma)} = -\frac{3}{2} \pm \sqrt{\tau} \,, \tag{39}$$

inasmuch as c_o can not be zero since it is the leading term in the series expansion. Once the roots of the indicial equation have been chosen, the succeeding equations uniquely determine the remaining coefficients (c_1 , c_2 , c_3 , . . . , c_n), provided the bracketed terms are not identically zero. The interpretation can be simplified by incorporating the values for α_1 (= - 3/2 + $\sqrt{\tau}$) and α_2(= - 3/2 - $\sqrt{\tau}$) into the general expression for the series, Eq. (34); the result is that the bracketed term for any specific value of n will be zero if either of the following equations are satisfied:

$$r^{\alpha_1}\left\{n\left(n+2\sqrt{\left(\frac{3}{2}\right)^2 - 2(1-\gamma)}\right)\right\} c_n r^{n-2} = 0 \quad \text{and} \tag{40}$$

$$r^{\alpha_2}\left\{n\left(n-2\sqrt{\left(\frac{3}{2}\right)^2 - 2(1-\gamma)}\right)\right\} c'_n r^{n-2} = 0 \,, \tag{41}$$

where the c'_n coefficients have been introduced solely to distinguish the individual series representations. If the bracketed term in either Eq. (40) or (41) is zero for any discrete value of γ , the corresponding coefficients (c_n or c'_n) are not defined and must be included in the series expansion for $T_{3(c)}$. To ensure that α is a real number, the quantity under the square root symbol must remain positive (the minimum value for γ is - 1/8). Therefore, Eq. (40) requires that all the c_n coeffieients be zero except c_o . On the other hand, Eq. (41) requires c'_o to be undefined, with the remaining coefficients (c'_n) being zero unless γ = 0 ($c'_1 \neq 0$), γ = 3/8 ($c'_2 \neq 0$), γ = 1 ($c'_3 \neq 0$), γ = 15/8 ($c'_4 \neq 0$), γ = 3 ($c'_5 \neq 0$), etc. For larger values of n, $\gamma >> 1$ for any coefficient to be undefined.

The values of γ treated in this text are not the same as any of the aforementioned values (except for the special case of isotropic material when γ = 1, which will be treated more thoroughly later in this section) and, thus, all the c'_n coefficients are zero except c'_o . As a result, for the anisotropic cases, the two distinct series that satisfy Eq. (33) with A_o = 0 are

$$T_{3(c)_1} = c_o r^{-\frac{3}{2}+\sqrt{\tau}} \quad \text{and} \quad T_{3(c)_2} = c_o' r^{-\frac{3}{2}-\sqrt{\tau}} \quad . \tag{42}$$

Therefore, the general complementary solution for the anisotropic cases can be written as

$$T_{3(c)} = c_o r^{-\frac{3}{2}+\sqrt{\tau}} + c_o' r^{-\frac{3}{2}-\sqrt{\tau}} \quad . \tag{43}$$

For the special case of $\gamma = 1$, which specifies that c_3' is undefined, the roots of the indicial equation become $a_1 = 0$ and $a_2 = -3$. The series solutions that evolve are, therefore,

$$T_{3(c)_1} = c_o \quad \text{and} \tag{44}$$

$$T_{3(c)_2} = r^{-3}\left(c_o' + c_3' r^3\right) = c_o' r^{-3} + c_3' \quad . \tag{45}$$

Since the constant term appearing in Eq. (44) is inherently contained in Eq. (45), the latter equation may be considered as an appropriate solution. For this particular case, since $a_1 - a_2 = 3$ is an integer, a second solution may be found by choosing as the general solution the function[3]

$$T_{3(c)} = A_1 T_{3(c)_2} + B_1\left(g_3 T_{3(c)_2} \ln r + \overline{T}_{3(c)}\right) \quad , \tag{46}$$

where

$$\overline{T}_{3(c)} = r^{-3}\left(-\frac{1}{3} + \sum_{n=1}^{\infty} h_n r^n\right)$$

and g_3 and the coefficients h_n are constants. Upon taking the first and second derivatives of Eq. (46) with respect to the radial coordinate and substituting these derivatives into Eq. (33), with $A_o = 0$ and $\gamma = 1$, we see that the following equation must be satisfied for Eq. (46) to be the general solution:

$$\frac{3g_3}{r^2}\left(c_3' - c_o' r^{-3}\right) + r^{-3} \sum_{n=1}^{\infty} n(n-3) h_n r^{n-2} = 0 \quad . \tag{47}$$

Now, since neither c_3' nor c_o' can be zero, Eq. (47) is satisfied only if $g_3 = 0$ and $h_n = 0$ for all $n \neq 3$. Therefore, the general solution may be written more explicitly as

$$T_{3(c)} = A_1 \left[c_o' r^{-3} + c_3'\right] + B_1 r^{-3} \left[-\frac{1}{3} + h_3 r^3\right] = r^{-3} \left[A_1 c_o' - \frac{B}{3}\right] + \left[A_1 c_3' + B_1 h_3\right] , \quad (48)$$

which degenerates to the form of Eq. (45), or Eq. (43) when $\gamma = 1$ ($\sqrt{\tau} = 3/2$). Consequently, Eq. (43) may be used as the general complementary solution for the radial stress distribution for the cases treated in this report.

The particular solution of Eq. (33) is easily found to be $T_{3(p)} = a_o/r^2$, where

$$a_o = -A_o \frac{(g_{31} + g_{33})}{(s_{13}^D + s_{33}^D)} . \quad (49)$$

Therefore, the complete solution for the radial stress can be written as

$$T_3 = \frac{a_o}{r^2} + c_o r^{-\frac{3}{2} + \sqrt{\tau}} + c_o' r^{-\frac{3}{2} - \sqrt{\tau}} . \quad (50)$$

In general, the radial stress is dependent upon the charge (q) through the constant A_o. However, since this analysis is concerned with determining the open-circuit sensitivity (q = 0), Eq. (50) simply reverts to Eq. (43).

Boundary conditions must now be imposed upon the radial stress distribution. These will be applied as follows:

a. The inside spherical surface at r = a will be considered to be completely free of any loading effects so that $T_3 = 0$, and

b. The outside spherical surface will be exposed to a uniform acoustic field so that $T_3 = -P_o$ at r = b (P_o is the acoustic pressure in dynes per square centimeter).

When these conditions are applied to the radial stress distribution, Eq. (50), with $a_o = 0$, then

$$c_o' = -c_o a^{2\sqrt{\tau}} \text{ and} \quad (51)$$

$$c_o = -\frac{P_o b^{\frac{3}{2} - \sqrt{\tau}}}{\left[1 - \left(\frac{a}{b}\right)^{2\sqrt{\tau}}\right]} . \quad (52)$$

Therefore, the principal stresses can be written in terms of the acoustic pressure as

$$T_3 = -P_o\left(\frac{b}{r}\right)^{\frac{3}{2}-\sqrt{\tau}} \frac{\left[1-\left(\frac{a}{r}\right)^{2\sqrt{\tau}}\right]}{\left[1-\left(\frac{a}{b}\right)^{2\sqrt{\tau}}\right]}, \tag{53}$$

and from Eq. (24),

$$T_1 = T_2 = -\frac{P_o}{2}\left(\frac{b}{r}\right)^{\frac{3}{2}-\sqrt{\tau}} \frac{\left\{\left(\frac{1}{2}+\sqrt{\tau}\right)-\left(\frac{a}{r}\right)^{2\sqrt{\tau}}\left(\frac{1}{2}-\sqrt{\tau}\right)\right\}}{\left[1-\left(\frac{a}{b}\right)^{2\sqrt{\tau}}\right]}. \tag{54}$$

When the material is isotropic, such that $\gamma = 1$ and $\sqrt{\tau} = 3/2$, the principal stresses reduce to those given by Roark[4]; i.e.,

$$T_3 = -P_o \frac{\left[1-\left(\frac{a}{r}\right)^3\right]}{\left[1-\left(\frac{a}{b}\right)^3\right]} \text{ and } T_1 = T_2 = -\frac{P_o}{2}\frac{\left[2+\left(\frac{a}{r}\right)^3\right]}{\left[1-\left(\frac{a}{b}\right)^3\right]}. \tag{55}$$

The open-circuit sensitivity (M_o) of hydrophone elements is defined as the ratio of the magnitude of the open-circuit voltage to the magnitude of the free-field acoustic pressure impinging upon the element. It should be noted that the sensitivities calculated herein are valid only for frequencies below and reasonably well removed from the lowest resonance frequency of the structure being considered. The first step in determining the sensitivity is to calculate the open-circuit voltage appearing between the electroded surfaces of the sphere. This is accomplished with the aid of Eq. (22) through the following formula:

$$V_{oc} = \int_a^b \mathcal{E}_3\, dr = \int_a^b \left[-2g_{31}T_1 - g_{33}T_3\right] dr. \tag{56}$$

Introducing Eqs. (53) and (54) into Eq. (56), integrating over the specified limits, and dividing the result by the free-field acoustic pressure yield

$$M_o = \frac{b}{\left[1-\left(\frac{a}{b}\right)^{2\sqrt{\tau}}\right]}\left\{g_{31}\left\{\frac{\left(\frac{1}{2}+\sqrt{\tau}\right)}{\left(\frac{1}{2}-\sqrt{\tau}\right)}\left[1-\left(\frac{a}{b}\right)^{-\frac{1}{2}+\sqrt{\tau}}\right]-\frac{\left(\frac{1}{2}-\sqrt{\tau}\right)}{\left(\frac{1}{2}+\sqrt{\tau}\right)}\left(\frac{a}{b}\right)^{2\sqrt{\tau}}\left[1-\left(\frac{a}{b}\right)^{-\frac{1}{2}-\sqrt{\tau}}\right]\right\}\right.$$

$$+ g_{33}\left\{\frac{1}{\left(\frac{1}{2}-\sqrt{\tau}\right)}\left[1-\left(\frac{a}{b}\right)^{-\frac{1}{2}+\sqrt{\tau}}\right]-\frac{\left(\frac{a}{b}\right)^{2\sqrt{\tau}}}{\left(\frac{1}{2}+\sqrt{\tau}\right)}\left[1-\left(\frac{a}{b}\right)^{-\frac{1}{2}-\sqrt{\tau}}\right]\right\}\right\} . \qquad (57)$$

For the isotropic case ($\sqrt{\tau} = 3/2$), Eq. (57) reduces to

$$M_o = \frac{b}{\left[1-\left(\frac{a}{b}\right)^3\right]}\left\{\frac{g_{31}}{2}\left[\left(\frac{a}{b}\right)^3+3\left(\frac{a}{b}\right)-4\right]+\frac{g_{33}}{2}\left[3\left(\frac{a}{b}\right)-\left(\frac{a}{b}\right)^3-2\right]\right\}, \qquad (58)$$

which agrees with Albers,[5] if his result is multiplied by the unit factor $[1 - (a/b)^3]/[1 - (a/b)]$. As the shell becomes very thin, $(a/b \longrightarrow 1)$, the sensitivity approaches the constant value

$$M_o = b g_{31} . \qquad (59)$$

This same result is achieved if Eq. (57) is evaluated in the limit as $a/b \longrightarrow 1$, which indicates that the anisotropic properties of the material have no effect on the sensitivity of very thin-walled spheres.

Since the preceding discussion was concerned solely with the analysis of hollow spheres that were pressure-released on the inside surface, it might be interesting to speculate on what variations may occur in the open-circuit sensitivities if the spherical ceramic elements were mechanically impeded on the inside surface instead of being free. A situation of this type can be envisioned if the ceramic is molded (or mounted) on a solid spherical body similar to the hydrophone design advocated by Barger and Hunt[6] for radially polarized cylindrical elements. This presentation will not attempt to define a procedure for achieving a physical representation of such a situation, but will simply exploit the theoretical advantages or disadvantages of such a situation.

In order to analyze a situation as described above, it will be assumed that the inside spherical surface of the ceramic is in immediate contact with the outside surface of a solid spherical body so that the radial stresses and particle displacements (u_r) of both bodies are continuous at that particular junction. Mathematically, these conditions are expressed as

$$T_{3_c} = T_{3_m} \text{ and } u_{r_c} = u_{r_m} \text{ at } r = a , \qquad (60)$$

where the subscripts c and m represent the ceramic and metal (solid core), respectively.

Since both bodies exhibit spherical symmetry, Eq. (43) may be used to express the radial stress distributions as

$$T_{3_c} = c_o r^{-\frac{3}{2}+\sqrt{\tau}} + c_o' r^{-\frac{3}{2}-\sqrt{\tau}} \quad \text{and} \tag{61}$$

$$T_{3_m} = d_1 + d_2 r^{-3} \quad , \tag{62}$$

where the last equation was formulated for an isotropic body ($\sqrt{\tau} = 3/2$).

Two additional boundary conditions must be imposed before proceeding with the analysis. First, the radial stress in the solid body at the origin of coordinates ($r = 0$) must be finite. Therefore, it is necessary at the outset to let $d_2 = 0$ so that the radial stress in the solid metal sphere becomes simply $T_{3_m} = d_1$. As far as the metallic body is concerned, Eqs. (23) and (24) require that the two transverse stresses be constant also: $T_{1_m} = T_{2_m} = T_{3_m} = d_1$. Second, the radial stress on the outside peripheral surface of the ceramic sphere must be equal to the impinging acoustic pressure, $-P_o$, such that $T_{3_c} = -P_o$ at $r = b$.

If these conditions, and those required by Eq. (60), are imposed upon Eqs. (61) and (62), it is easily verified that the following relationships must hold:

$$c_o = \frac{-P_o b^{\frac{3}{2}-\sqrt{\tau}}}{\left[1 - \left(\frac{a}{b}\right)^{2\sqrt{\tau}} \frac{(G_+ - 1)}{(G_- - 1)}\right]} , \tag{63}$$

$$c_o' = \frac{P_o a^{2\sqrt{\tau}} b^{\frac{3}{2}-\sqrt{\tau}} \frac{(G_+ - 1)}{(G_- - 1)}}{\left[1 - \left(\frac{a}{b}\right)^{2\sqrt{\tau}} \frac{(G_+ - 1)}{(G_- - 1)}\right]} \quad , \text{ and} \tag{64}$$

$$d_1 = \frac{-P_o \left(\frac{a}{b}\right)^{-\frac{3}{2}+\sqrt{\tau}} \frac{(G_- - G_+)}{(G_- - 1)}}{\left[1 - \left(\frac{a}{b}\right)^{2\sqrt{\tau}} \frac{(G_+ - 1)}{(G_- - 1)}\right]} . \tag{65}$$

where

$$G_+ = \frac{s_{13}^D + \frac{s_{11}^D}{2}(1-\sigma^D)\left(\frac{1}{2}+\sqrt{\tau}\right)}{s_{11_m}(1-2\sigma_m)} \text{ and} \tag{66}$$

$$G_- = \frac{s_{13}^D + \frac{s_{11}^D}{2}(1-\sigma^D)\left(\frac{1}{2}-\sqrt{\tau}\right)}{s_{11_m}(1-2\sigma_m)} \quad . \tag{67}$$

In the two preceding equations, s_{11_m} is the uniaxial compliance coefficient for the metallic material, $\sigma_m = -s_{12_m}/s_{11_m}$, and $\sigma^D = -s_{12}^D/s_{11}^D$ (σ_m and σ^D are Poisson's ratios). As a matter of interest, note that the following definitions for the radial particle displacements were used in evaluating the preceeding G constants:

$$u_{r_c} = c_o r^{-\frac{1}{2}+\sqrt{\tau}}\left[s_{13}^D + \frac{s_{11}^D}{2}(1-\sigma^D)\left(\frac{1}{2}+\sqrt{\tau}\right)\right] + c_o' r^{-\frac{1}{2}-\sqrt{\tau}}\left[s_{13}^D + \frac{s_{11}^D}{2}(1-\sigma^D)\left(\frac{1}{2}-\sqrt{\tau}\right)\right] \text{ and} \tag{68}$$

$$u_{r_m} = r d_1 s_{11_m}(1-2\sigma_m) \quad . \tag{69}$$

Now, if Eq. (56) is used to define the open-circuit voltage appearing between the electroded surfaces of the ceramic, in conjunction with Eqs. (61) and (24), with T replaced by T_c, and if the indicated integration is carried out, then

$$V_{oc} = -2g_{31}\left\{\frac{c_o\left(\frac{1}{2}+\sqrt{\tau}\right)}{2\left(-\frac{1}{2}+\sqrt{\tau}\right)} b^{-\frac{1}{2}+\sqrt{\tau}}\left[1-\left(\frac{a}{b}\right)^{-\frac{1}{2}+\sqrt{\tau}}\right] + \frac{c_o'\left(\frac{1}{2}-\sqrt{\tau}\right)}{2\left(-\frac{1}{2}-\sqrt{\tau}\right)} b^{-\frac{1}{2}-\sqrt{\tau}}\left[1-\left(\frac{a}{b}\right)^{-\frac{1}{2}-\sqrt{\tau}}\right]\right\}$$

$$-g_{33}\left\{\frac{c_o b^{-\frac{1}{2}+\sqrt{\tau}}}{\left(-\frac{1}{2}+\sqrt{\tau}\right)}\left[1-\left(\frac{a}{b}\right)^{-\frac{1}{2}+\sqrt{\tau}}\right] + \frac{c_o' b^{-\frac{1}{2}-\sqrt{\tau}}}{\left(-\frac{1}{2}-\sqrt{\tau}\right)}\left[1-\left(\frac{a}{b}\right)^{-\frac{1}{2}-\sqrt{\tau}}\right]\right\} \quad . \tag{70}$$

Using the standard definition of the open-circuit sensitivity, we can easily verify that

$$M_o = \frac{b}{\left[1-\left(\frac{a}{b}\right)^{2\sqrt{\tau}}\frac{(G_+-1)}{(G_--1)}\right]}\left\{g_{31}\left\{\frac{\left(\frac{1}{2}+\sqrt{\tau}\right)}{\left(\frac{1}{2}-\sqrt{\tau}\right)}\left[1-\left(\frac{a}{b}\right)^{-\frac{1}{2}+\sqrt{\tau}}\right] - \left(\frac{a}{b}\right)^{2\sqrt{\tau}}\frac{\left(\frac{1}{2}-\sqrt{\tau}\right)}{\left(\frac{1}{2}+\sqrt{\tau}\right)}\left[1-\left(\frac{a}{b}\right)^{-\frac{1}{2}-\sqrt{\tau}}\right]\frac{(G_+-1)}{(G_--1)}\right\}\right.$$

$$+ g_{33}\left\{\frac{\left[1-\left(\frac{a}{b}\right)^{-\frac{1}{2}+\sqrt{\tau}}\right]}{\left(\frac{1}{2}-\sqrt{\tau}\right)} - \frac{\left(\frac{a}{b}\right)^{2\sqrt{\tau}}\left[1-\left(\frac{a}{b}\right)^{-\frac{1}{2}-\sqrt{\tau}}\right]}{\left(\frac{1}{2}+\sqrt{\tau}\right)}\frac{(G_+-1)}{(G_--1)}\right\}\right\}. \qquad (71)$$

When the metallic body disappears ($s_{11_m} \to \infty$), the multiplying factor, $(G_+ - 1)/(G_- - 1)$, approaches unity and Eq. (71) reverts to Eq. (57). But when the metallic body is infinitely stiff ($s_{11_m} \to 0$), the multiplying factor becomes

$$\frac{G_+ - 1}{G_- - 1} = \frac{s^D_{13} + \frac{s^D_{11}}{2}(1-\sigma^D)\left(\frac{1}{2}+\sqrt{\tau}\right)}{s^D_{13} + \frac{s^D_{11}}{2}(1-\sigma^D)\left(\frac{1}{2}-\sqrt{\tau}\right)}. \qquad (72)$$

The information contained in Eqs. (57) and (71) is depicted in Figs. 2 through 4 in the form of $M_o/2b$ (open-circuit sensitivity in μvolts per μbar per inch diameter) versus the ratio, R = (b - a)/2b, of wall thickness to outside diameter for the ceramic materials that are currently being used in hydrophone designs. As is easily recognized from the graphs, the anisotropic characteristics of the ceramic materials have a negligible effect on the open-circuit sensitivities when compared with similar sensitivities derived using stress distributions that obey isotropic criteria. The exception was in the region of zero sensitivity — a region of no practical importance. In Figs. 2 through 4, the values of the ceramic properties were taken from published data[7] and are listed in Table 1. The graphs presented in Fig. 5 for the lead-metaniobate ceramic are based solely on the isotropic formulization because of the unavailability of all the necessary material parameters for this particular ceramic. The piezoelectric coefficients, $g_{31} = -7.0 \times 10^{-3}$ (v - m)/N and $g_{33} = 40 \times 10^{-3}$ (v - m)/N, for the lead-metaniobate ceramic were taken from a commercial pamphlet.[8]

It is readily discernible from Figs. 2 through 5 that the maximum sensitivity for a thin-walled hollow polarized ferroelectric ceramic sphere is exhibited by PZT-5A ceramic. Although the PZT-5A and PZT-4 ceramics have a comparable value, the roll-off in sensitivity versus wall thickness is less severe for the PZT-5A, and, therefore, should be less dependent on dimensional tolerances.

Table 1

MATERIAL PROPERTIES OF CERAMICS

Parameters	Ceramic Materials		
	Ceramic B	PZT-4	PZT-5A
g_{31}	$-5.5 \times 10^{-3} \frac{v-m}{N}$	$-11.1 \times 10^{-3} \frac{v-m}{N}$	$-11.4 \times 10^{-3} \frac{v-m}{N}$
g_{33}	$14.1 \times 10^{-3} \frac{v-m}{N}$	$26.1 \times 10^{-3} \frac{v-m}{N}$	$24.8 \times 10^{-3} \frac{v-m}{N}$
s_{33}^D/s_{11}^D	.843	.725	.657
$s_{12}^D/s_{11}^D = -\sigma^D$	-.349	-.497	-.535
s_{13}^D/s_{33}^D	-.271	-.266	-.315
$\gamma = \frac{s_{33}^D\left(1 + s_{13}^D/s_{33}^D\right)}{s_{11}^D\left(1 + s_{12}^D/s_{11}^D\right)}$	.945	1.058	.968
$\sqrt{\gamma}$	1.463	1.538	1.479
$\frac{(G_+ - 1)}{(G_- - 1)}_{s_{11_m} = 0}$	-.755	-.705	-.582
$\frac{(G_+ - 1)}{(G_- - 1)}_{s_{11_m} = 5.13 \times 10^{-12} \frac{m^2}{N}}$	-.206	-.205	-.192

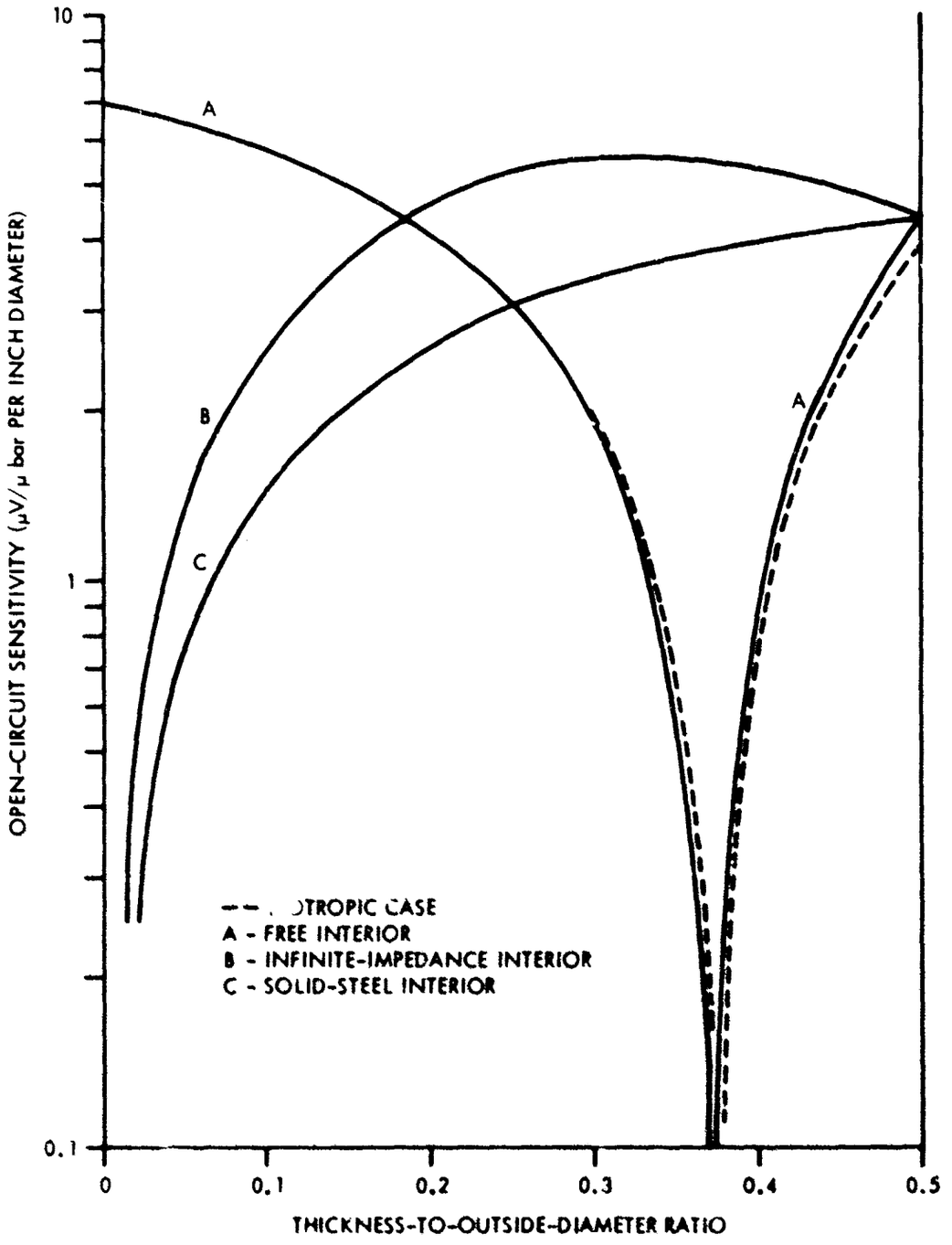

Fig. 2. Open-Circuit Sensitivity versus Thickness-to-Outside-Diameter Ratio of a Radially Polarized Ceramic B Sphere

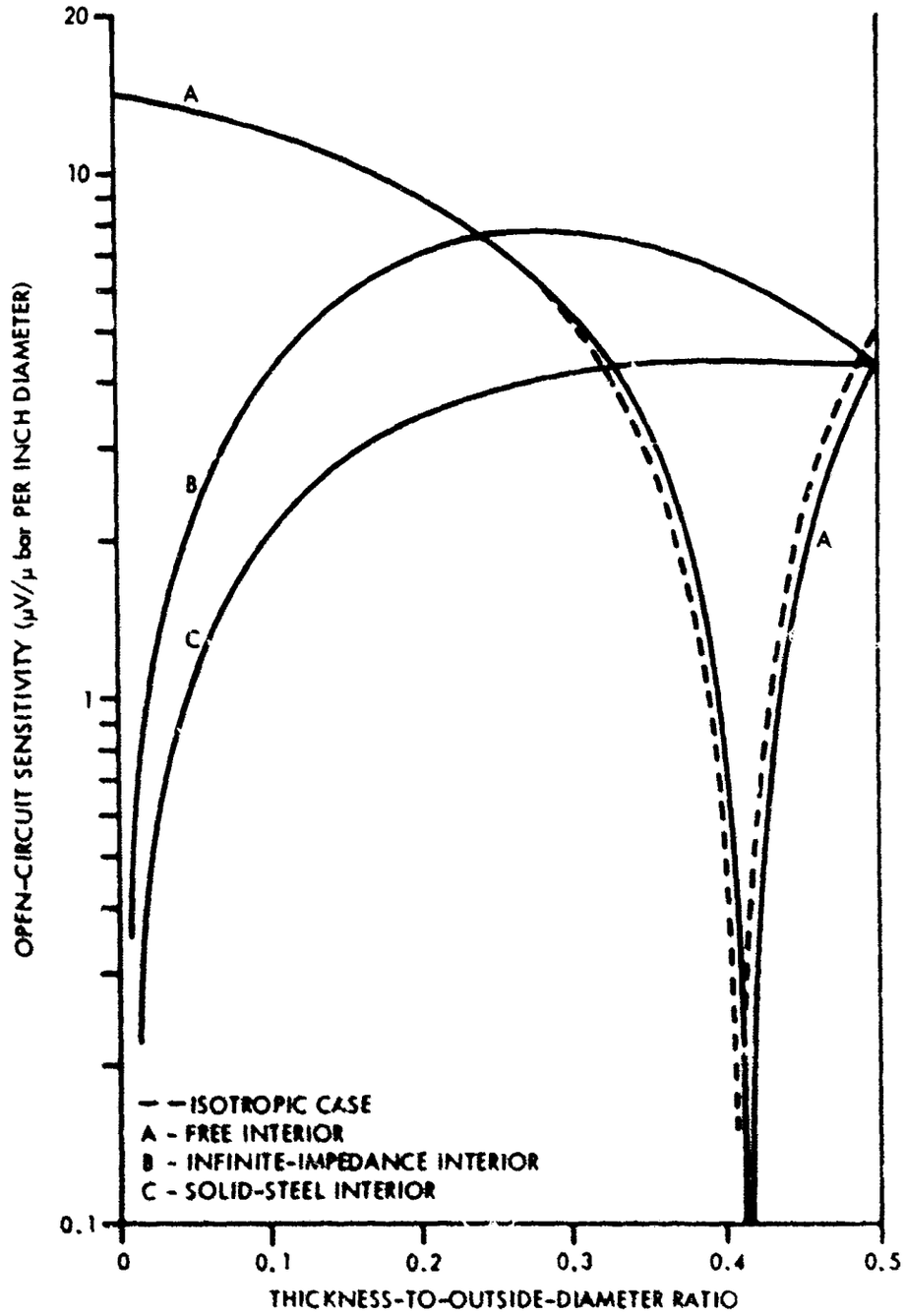

Fig. 3. Open-Circuit Sensitivity versus Thickness-to-Outside-Diameter Ratio of a Radially Polarized PZT-4 Sphere

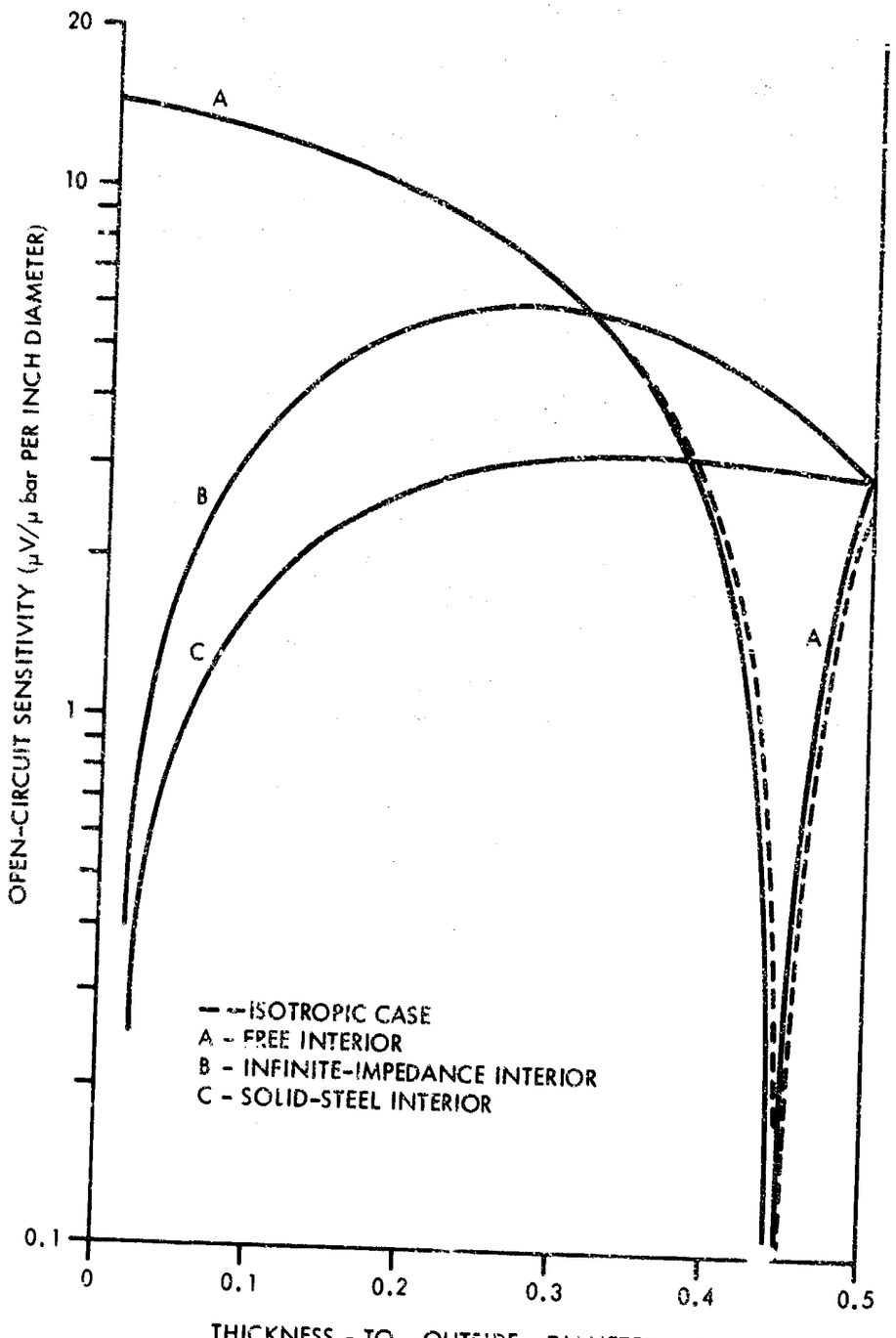

Fig. 4. Open-Circuit Sensitivity versus Thickness-to-Outside-Diameter Ratio of a Radially Polarized PZT-5A Sphere

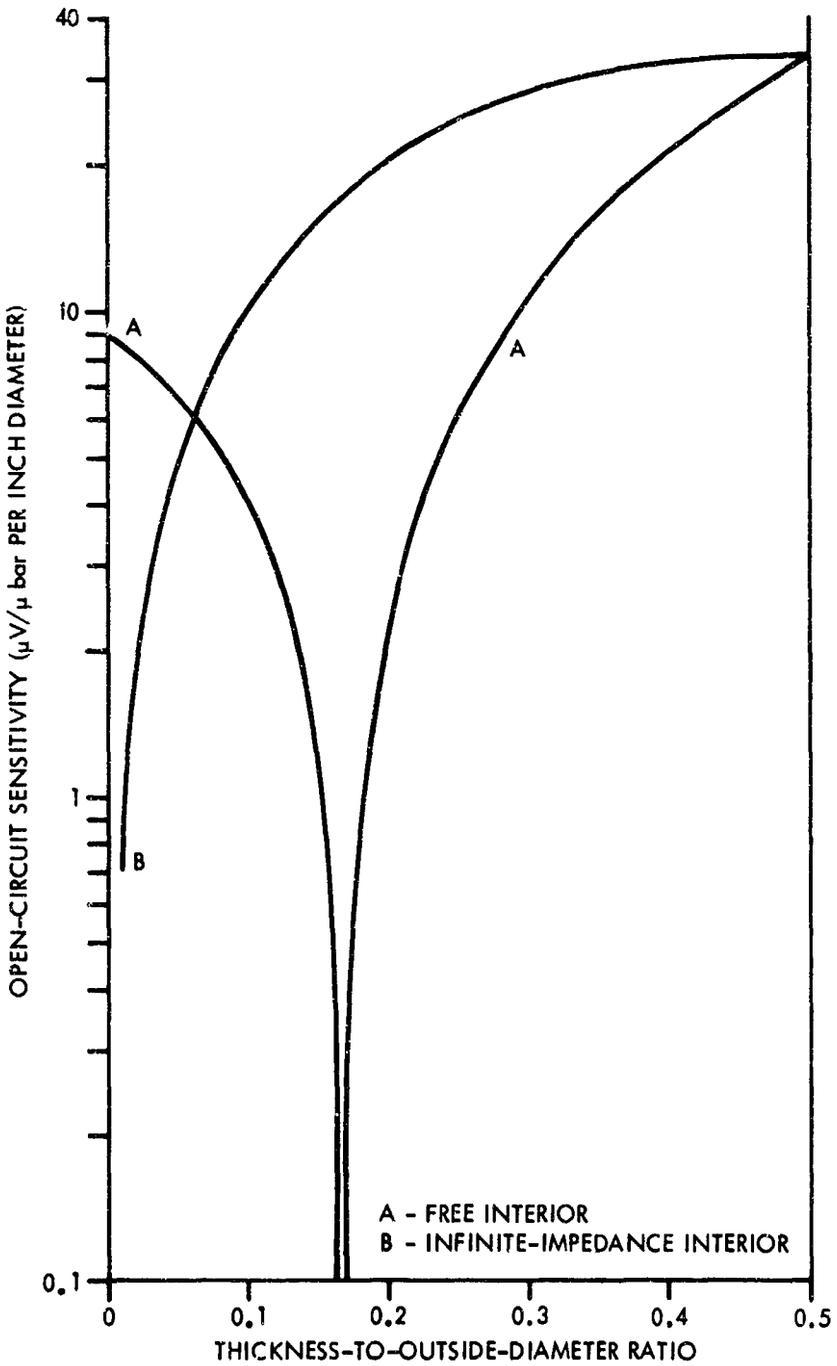

Fig. 5. Open-Circuit Sensitivity versus Thickness-to-Outside-Diameter Ratio of a Radially Polarized Lead-Metaniobate Sphere

For comparative purposes, Figs. 2 through 5 include the limiting case of an infinitely stiff solid core, which is designated by the symbol B. These cases symbolize the ideal maximum sensitivities that can be achieved with a solid core. The main disadvantage in the design of solid-core hydrophones is apparent from the graphs, i.e., the sensitivities that can be obtained are lower than those that can be achieved with thin-walled spheres completely free on the inside surface. As the stiffness of the insert diminishes, the sensitivity decreases also. This statement is clarified by referring to the plots, labeled C in Figs. 2 through 4, that show the sensitivity of spherical ceramic elements when the infinitely stiff solid core is replaced by a steel insert with a finite stiffness. The parameters for the steel were chosen to be $\sigma_m = 0.3$ and $s_{11_m} = 5.13 \times 10^{-12}$ m^2/N [Young's modulus $(Y_{11_m}) = 28.3 \times 10^6$ psi].

Although the sensitivity of infinitely stiff, solid-core devices can approach the sensitivity of pressure-released devices, e.g., Ceramic B, this is only accomplished for relatively thick-walled ceramic bodies. The only case where solid-core design seems beneficial is in conjunction with the lead-metaniobate ceramic. However, for these cases, it should be noted that problems might arise in trying to uniformly polarize such thick spherical elements. In addition, there are the very practical problems associated with constructing such a design, e.g., mounting the active ceramic on the solid core, bonding (if necessary), as well as increasing the weight of the complete element because of the insert. These disadvantages negate the practical advantages of increasing the fundamental resonance of the element and enhancing the unit's resistance to shock damage.

The stresses induced in a hollow ceramic sphere (unloaded on the inside spherical surface) because of the ambient hydrostatic pressure (P_h) can be expressed by Eqs. (53) and (54) if P_o is replaced by P_h. The magnitude of the radial stress, described by Eq. (53), is plotted in Fig. 6 as a function of the radial coordinate for various values of the ratio of inside to outside radius. The three cases represented in Fig. 6 are for the anisotropy parameter (γ) greater than and less than unity and for γ equal to unity (isotropic). When $a/b \geq 0.4$, the values for the radial stress in the three cases are roughly equal and are represented by a single curve for each distinct a/b ratio. However, when $a/b < 0.4$, there is a definite difference in the magnitude of the radial stress for the three cases. It is apparent from Fig. 6 that

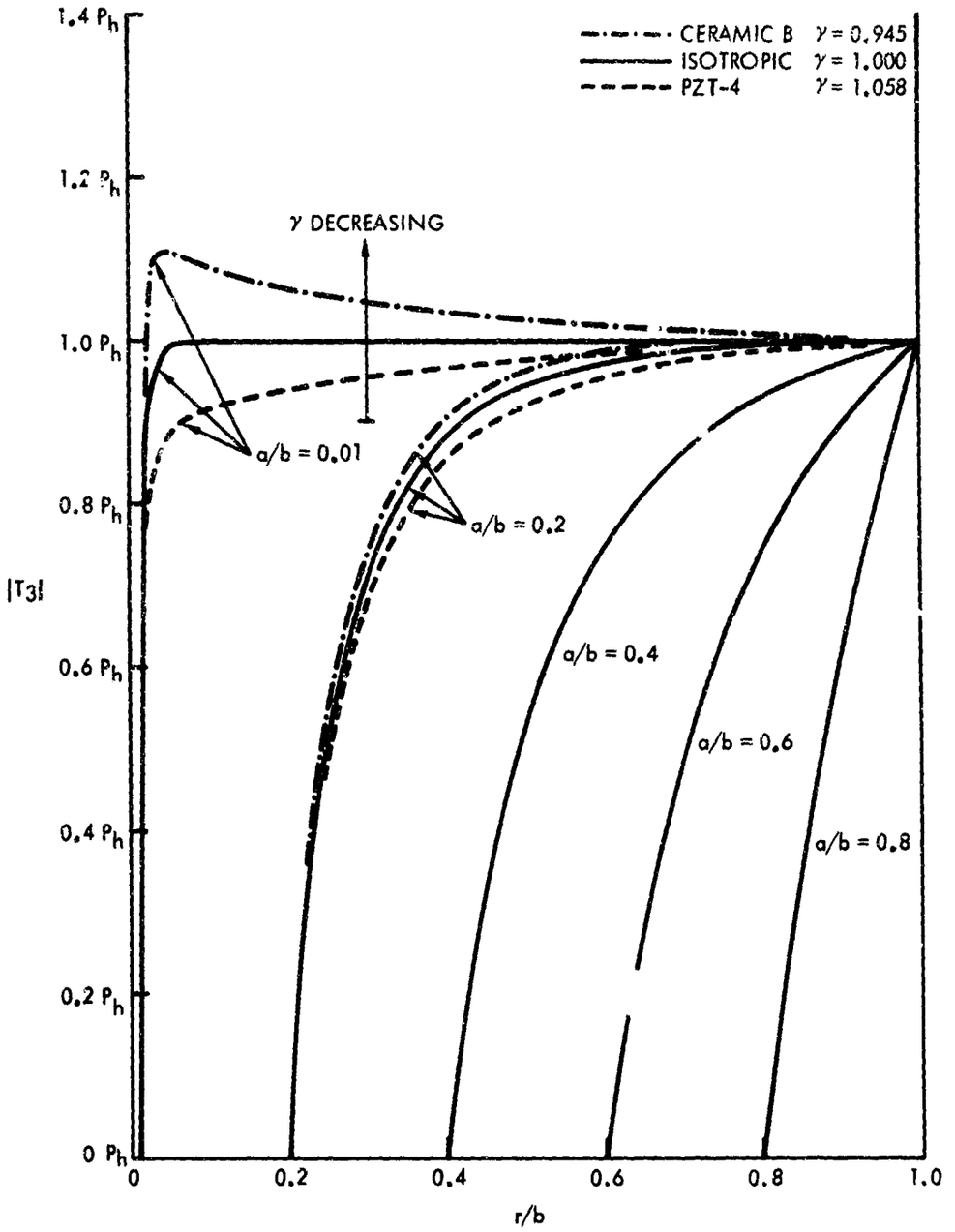

Fig. 6. Magnitude of the Radial Stress versus the Radial Coordinate for Various Ratios of Inside-to-Outside Radius

this difference increases rapidly as the ratio a/b approaches zero. The peak value of the radial stress for Ceramic B ($\gamma < 1.0$) tends toward a very large number as a/b becomes very small, whereas the radial stress for PZT-4 ceramic ($\gamma > 1.0$) tends toward zero as a/b becomes very small. Figure 7 is a plot of the magnitude of Eq. (53) for the limiting case of a/b = 0:

$$|T_3| = P_h\left(\frac{b}{r}\right)^{\frac{3}{2}-\sqrt{\tau}} \quad . \tag{73}$$

When $\gamma = 1$ ($\sqrt{\tau} = 3/2$), the radial stress for the isotropic case is well behaved and is constant, as expected. This result agrees with the derivation of the radial stress distribution for a solid sphere as determined using Eq. (43) with $\sqrt{\tau} = 3/2$ and $T_{3(c)} = T_3$:

$$T_3 = c_o + c_o' r^{-3} \quad . \tag{74}$$

Since T_3 is assumed to be finite at the origin (r = 0) of the coordinate system, the standard procedure is to set the coefficient c_o' equal identically to zero. Therefore, the boundary condition that stipulates that the radial stress at the outside spherical surface (r = b) be continuous with the applied load (P_h) requires that T_3 be constant and equal to P_h throughout the body, as depicted in Fig. 7.

However, when the anisotropic characteristics of the ceramic are considered and their effects are included in the solution for the radial stress, Eq. (73) may take either of two forms, one for $\sqrt{\tau} > 3/2$ and the other for $\sqrt{\tau} < 3/2$. The former case is exemplified by PZT-4 ceramic, and the latter case is exemplified by Ceramic B (or PZT-5A). As shown in Fig. 7, when $\sqrt{\tau} > 3/2$ (or equivalently, when $\gamma > 1.0$), the radial stress diminishes to zero as $r \to 0$; however, when $\sqrt{\tau} < 3/2$, the radial stress becomes infinite as $r \to 0$. The latter situation is not commensurate with the practical realization that the radial stress should be finite at the origin of a spherical solid body. Nevertheless, even though the radial stress distribution might be considered to fail for the limiting case of a solid sphere, it should be satisfactory for all cases that contain a hole with finite dimensions centered about the origin.

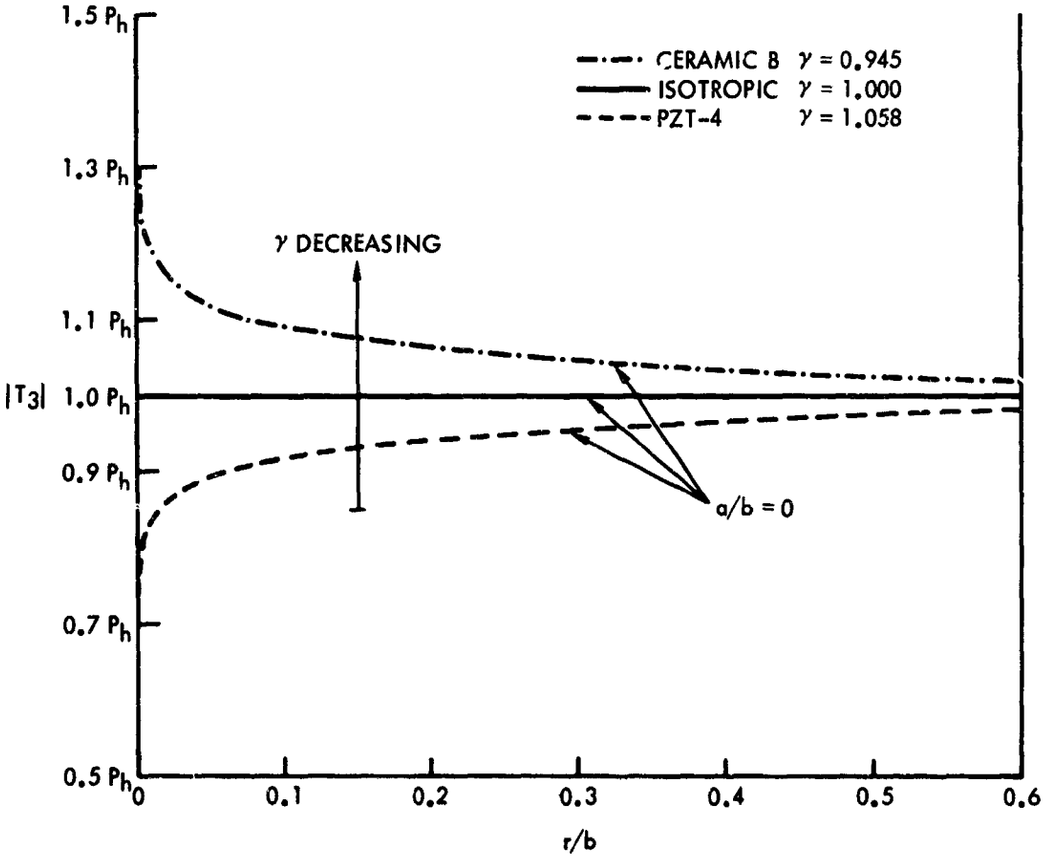

Fig. 7. Magnitude of the Radial Stress versus the Radial Coordinate for the Limiting Case of a Solid Sphere

Figure 8 depicts the magnitude of the polar stress, T_1, as a function of the radial coordinate for various values of the ratio a/b. The lines connecting the innermost stress values for distinct a/b ratios represent the envelopes of the maximum stresses experienced by hollow spheres for the three kinds of isotropy treated herein. Note that here again the stress tends to become very large, stable at P_h, or very small, depending on the value of the anisotropy parameter, as a/b becomes very small. The limiting case for a/b = 0 can be inferred from Fig. 7 for the magnitude of the polar stress by referring to the following formula:

$$|T_1| = \frac{1}{2} P_h \left(\frac{b}{r}\right)^{\frac{3}{2}-\sqrt{\tau}} \left(\frac{1}{2}+\sqrt{\tau}\right) . \tag{75}$$

The phenomenon associated with the radial stress when the anisotropy parameter is less than unity appears to be limited to radially polarized ceramic elements. A similar type of phenomenon was encountered in the investigation of the open-circuit sensitivities of radially polarized ferroelectric ceramic cylinders.[9] Undoubtedly, these phenomena are related to the types of material symmetry induced in the spherical and cylindrical ceramic elements by radial polarization. As a matter of academic interest, the relationship between the spherical and cylindrical anisotropy parameters is

$$\gamma = \frac{s_{33}^D \left(1 + s_{13}^D / s_{33}^D\right)}{s_{11}^D \left(1 + s_{12}^D / s_{11}^D\right)} , \tag{76}$$

where s_{33}^D / s_{11}^D is the cylindrical anisotropy parameter of the ceramic when it is used as a hydrophone element.

The preceding derivation for the induced stresses in a sphere as a result of ambient hydrostatic pressure indicates that the predicted internal stresses for certain types of material anisotropy are not realizable for solid configurations. As a means of overcoming this barrier, it would be instructive to seek a realistic approach to the problem. Consider, for example, the very practical fact that in order to radially polarize a ceramic sphere it is essential that a finite hole be maintained about the origin of the coordinate system to introduce the inside electrode.* In the limiting case, the hole may be completely

*Similar reasoning can be employed for the case of radially polarized ceramic cylinders.

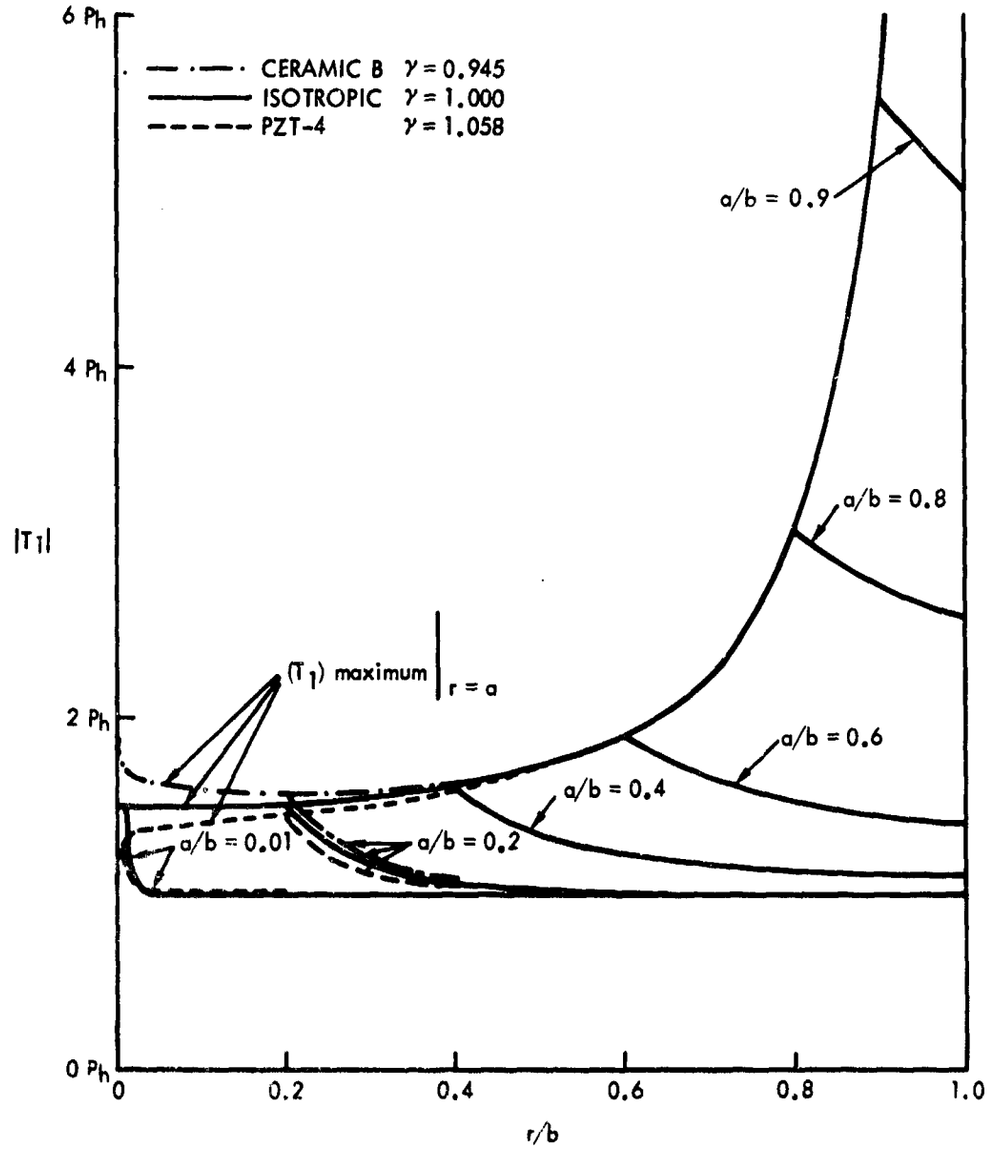

Fig. 8. Magnitude of the Polar Stress versus the Radial Coordinate for Various Ratios of Inside-to-Outside Radius

filled with the electrode material. In this case, the composite sphere may be considered to be a ceramic sphere mounted on a solid sphere. Consequently, Eqs. (61) and (62) can be used to derive the complete radial stress distribution. Using the relationships expressed in Eqs. (63) through (65), with P_o replaced by P_h, $d_2 = 0$, and $\underline{a}$ replaced by ϵ (some small finite distance), we can express the radial stresses in both spherical bodies as

$$T_{3_c} = \frac{-P_h\left(\frac{b}{r}\right)^{\frac{3}{2}-\sqrt{\tau}}}{\left[1-\left(\frac{\epsilon}{b}\right)^{2\sqrt{\tau}}\frac{(G_+-1)}{(G_--1)}\right]}\left\{1-\left(\frac{\epsilon}{r}\right)^{2\sqrt{\tau}}\frac{(G_+-1)}{(G_--1)}\right\} \text{ for } \epsilon \leq r \leq b \text{ and} \tag{77}$$

$$T_{3_m} = \frac{-P_h\left(\frac{\epsilon}{b}\right)^{-\frac{3}{2}+\sqrt{\tau}}\frac{(G_--G_+)}{(G_--1)}}{\left[1-\left(\frac{\epsilon}{b}\right)^{2\sqrt{\tau}}\frac{(G_+-1)}{(G_--1)}\right]} \text{ for } 0 \leq r \leq \epsilon \ . \tag{78}$$

Since ϵ can not be zero, Eq. (78) gives the limiting value of the radial stress in terms of the ambient pressure for any value of the anisotropy parameter and the dimensions and properties of the electrode. If the ceramic is stress-limited by the maximum allowable stress (maintained) parallel to the polar axis, Eq. (78) would give the maximum static pressure that could be sustained by the composite sphere, or the minimum electrode dimension that would not allow depolarization of the ceramic because of static pressure.

A similar expression for the transverse stresses in the ceramic can be derived using Eqs. (24) and (77), if these are the limiting stresses, namely,

$$T_{1_c} = \frac{-\left(\frac{1}{2}+\sqrt{\tau}\right)P_h\left(\frac{b}{\epsilon}\right)^{\frac{3}{2}-\sqrt{\tau}}}{2\left[1-\left(\frac{\epsilon}{b}\right)^{2\sqrt{\tau}}\frac{(G_+-1)}{(G_--1)}\right]}\left\{1-\frac{\left(\frac{1}{2}-\sqrt{\tau}\right)}{\left(\frac{1}{2}+\sqrt{\tau}\right)}\frac{(G_+-1)}{(G_--1)}\right\}, \text{ at } r=\epsilon \ . \tag{79}$$

Although the phenomenon associated with the induced stresses in very thick-walled hollow spheres is purely of academic interest (spherical hydrophone elements are designed so that the ratio a/b is ≥ 0.75), the investigation demonstrated the importance of keeping the anisotropic properties of ceramic materials in the analysis in order to account for any possible discrepancies that might occur.

It should be recognized that the preceding discussion was based on the assumption that the ceramic behaved as a homogeneous body. In practice, however, homogeniety can not be realized on account of the impossibility of poling the sphere equally throughout with a spherically divergent field. In effect, this means that for thick-walled spheres there will be a substantial gradient of elasto-dielectric properties.[10] A similar type of inhomogeniety exists for thick, radially poled cylinders, but it is not as severe as it is for spheres.

COMMENTS

The open-circuit sensitivities of radially polarized hollow spheres of several different ferroelectric ceramics that include the anisotropic characteristics of the material have been determined. The ensuing results were found to agree with corresponding sensitivities of hollow spheres that were determined using formulas for the internal stresses that obeyed isotropic criteria (biharmonic equation). For the cases of practical interest — thin-walled hollow spheres — the agreement was especially good.

The overall maximum sensitivity for thin-walled spheres was achieved with the PZT-5A ceramic, although the PZT-4 ceramic was in very close contention. The data in Fig. 5 demonstrate that thin-walled hollow spheres of lead metaniobate are not conducive to good hydrophone design because of the fast roll-off in sensitivity in the region of small values of R (ratio of wall thickness to outside diameter). However, as also depicted in Fig. 5, the sensitivity of the lead metaniobate can be enhanced to the point of being comparable to the sensitivities of the other ceramics (for relatively small values of wall thickness) by inserting a very stiff metallic body in the hollow space of the sphere in immediate contact with the ceramic. This technique has disadvantages as outlined earlier.

The investigation of the internal shell stresses induced in polarized ferroelectric ceramic spheres by ambient hydrostatic loads uncovered some strange phenomena. When the anisotropy parameter (γ) is greater than unity, the radial and transverse stresses are somewhat lower than the isotropic stresses for equivalent values of the radial coordinate (r/b), especially when the wall thickness becomes large

($a/b \to 0$, or $R \to 0.5$). In the limit of a solid body for this case, the anisotropic stresses approach zero as $r \to a$ (the inside radius). However, when the anisotropy parameter is less than unity, the internal stresses are slightly larger than the isotropic stresses and, in the limit of a solid body, approach large values as $r \to a$. In essence, this means that for the particular type of anisotropy that has large stresses (much greater than the ambient load) there is a limiting value for the dimensions of the interior hole that must be maintained if the sphere is to have the capacity to resist mechanical breakdown. It should be noted again, however, that the phenomenon associated with the internal stresses for thick-walled spheres is purely of academic interest since all practical hydrophone desig that utilize spherical elements are based on thin-wall criteria.

LIST OF REFERENCES

1. A. E. H. Love. A Treatise on the Mathematical Theory of Elasticity, Dover Publications, New York (4th edition), 1927, p. 54.

2. Ibid, p. 91.

3. E. T. Whittaker and G. N. Watson, A Course of Modern Analysis, Cambridge University Press, New York (4th edition), 1963, p. 201.

4. R. J. Roark, Formulas for Stress and Strain, McGraw-Hill Book Co., Inc., New York, 1954, p. 276.

5. V. M. Albers, editor, Underwater Acoustics, Plenum Press, New York, 1961, p. 20.

6. J. E. Barger and F. V. Hunt, "Solid-Core Probe Hydrophone," Journal of the Acoustical Society of America, vol. 36, no. 8, August 1964, p. 1589.

7. W. P. Mason, editor, Physical Acoustics, vol. I, part A, Academic Press, New York, 1964, p. 202.

8. "Kézite Lead Methaniobate Ceramic K-80," Bulletin 6901, Karamos, Inc., Azusa, Calif., February 1969.

9. C. L. LeBlanc, The Open-Circuit Sensitivity of Radially Polarized Ferroelectric Ceramic Cylinders, NUSC Report No. NL-4001, 18 September 1970.

10. H. Jaffe, F. Rosenthal, and H. Baerwald, Research and Development of Spherical Transducers, Clevite Research Center Final Development Report, April 1957 (ONR Contract Nonr 1825(00)).

REVERSE BLANK

UNCLASSIFIED

Security Classification

DOCUMENT CONTROL DATA - R & D

Security classification of title, body of abstract and indexing annotation must be entered when the overall report is classified)

1. ORIGINATING ACTIVITY (Corporate author)	2a. REPORT SECURITY CLASSIFICATION
New London Laboratory Naval Underwater Systems Center New London, Connecticut 06320	UNCLASSIFIED 2b. GROUP

3. REPORT TITLE

THE OPEN-CIRCUIT SENSITIVITY OF RADIALLY POLARIZED FERROELECTRIC CERAMIC HOLLOW SPHERES

4. DESCRIPTIVE NOTES (Type of report and inclusive dates)

Research Report

5. AUTHOR(S) (First name, middle initial, last name)

Charles L. LeBlanc

6. REPORT DATE	7a. TOTAL NO. OF PAGES	7b. NO. OF REFS
14 December 1970	36	10

8a. CONTRACT OR GRANT NO	9a. ORIGINATOR'S REPORT NUMBER(S)
b. PROJECT NO A-509-00-00	NL-3030
c. SF 35 452 007-12970	9b. OTHER REPORT NO(S) (Any other numbers that may be assigned this report)
d. (Partial)	

10. DISTRIBUTION STATEMENT

This document has been approved for public release and sale; its distribution is unlimited.

11. SUPPLEMENTARY NOTES	12. SPONSORING MILITARY ACTIVITY
	Department of the Navy

13. ABSTRACT

The open-circuit sensitivities of radially polarized ferroelectric ceramic spheres are derived from the viewpoint of treating the ceramic as an anisotropic material. The results are in good agreement with similar sensitivities predicted on the basis of isotropic stress distributions. Graphs of the open-circuit sensitivity versus the ratio of wall thickness to outside diameter for several different ceramic materials indicate the region over which the spherical elements may be considered to be thin-walled spheres. Included for comparison are the sensitivities of similar ceramic spheres that are not pressure-released on the inside surface but are in immediate contact with a solid sphere. Also included are graphs of the magnitude of the stresses induced in the spheres by the ambient hydrostatic pressures.

DD FORM 1 NOV 65 1473 (PAGE 1)

S/N 0102-014-6600

UNCLASSIFIED

Security Classification

14 KEY WORDS	LINK A		LINK B		LINK C	
	ROLE	WT	ROLE	WT	ROLE	WT
Ambient Hydrostatic Pressure						
Anisotropic Material						
Isotropic Stress Distributions						
Open-Circuit Sensitivity						
Radially Polarized Ferroelectric Ceramic Hollow Spheres						